Prediction of the Mean Diameter of Particle-Cluster Fractal Soot Aggregates Formed Inside Envelope Droplet Flames

Ben-Dor G., Elperin T. and Krasovitov B.

Department of Mechanical Engineering, The Pearlstone Center for Aeronautical Engineering Studies, Ben-Gurion University of the Negev, P.O.B. 653, Beer-Sheva 84105, ISRAEL

Numerical analysis of the effects of thermo- and diffusiophoretic forces on motion of particle-cluster (P-C) fractal soot aggregates and formation of soot shell structure in the buoyant-free envelope droplet flames is performed. It was shown that the P-C fractal soot aggregates are accumulated between the droplet surface and the flame front. The dependence of the soot-shell-to-droplet diameter ratios (d_s/d) on the mean radii of fractal soot aggregates was calculated numerically. Comparing the dependences of soot-shell-to-droplet diameter ratio on time calculated using the present model with the available experimental data for 0.63mm n-heptane droplet allowed us to determine the time dependence of the mean P-C soot aggregates radii. It was found that during droplet combustion the mean soot aggregates size grows slowly and linearly with time.

1. Introduction

During fuel droplet combustion temperature and concentration distributions in the neighborhood of a droplet are highly inhomogeneous. In this case the thermo- and diffusiophoretic forces caused by temperature and concentration gradients affect the soot aggregates located in the neighborhood of the burning droplets. In spherically symmetric droplet flames the effects of thermo- and diffusiophoresis lead to the soot aggregates accumulation between the droplet and the flame front [2], [3].
The location of combustion-generated aggregates between the droplet and the flame front is determined by the balance between the inwardly directed thermophoretic forces and outwardly directed drag forces and diffusiophoretic forces which act on soot aggregates formed during combustion of sooting fuel droplets. Outside the flame front soot aggregates move away from the flame front.
Flame-generated aggregates formed during droplet combustion have fairly complex morphology. However, the structure of flame-generated aggregates shows some evidence of fractal-like properties. The latter can simplify their morphological description as it was demonstrated experimentally and supported by several theoretical studies [4], [8].

2. Formation of fractal soot aggregates and soot accumulation inside envelope droplet flames

The production of soot particles in a flame is a chemically controlled process. Initial size of the soot particles is of the order of 10–30 nm. However, when soot particles are formed, they grow fast by surface growth and collisional coagulation. At the earlier stage of droplet combustion soot particles form cluster-cluster (C-C) fractal aggregates with a fractal dimension (D_f ~1.59 – 1.61). Then these aggregates may undergo the restructuring process whereby their open branched structure collapses resulting in a more compact cluster (see Fig. 1.), i.e., particle-cluster (P-C) fractal aggregates with large fractal dimension ($D_f \approx 2.75$) [4].

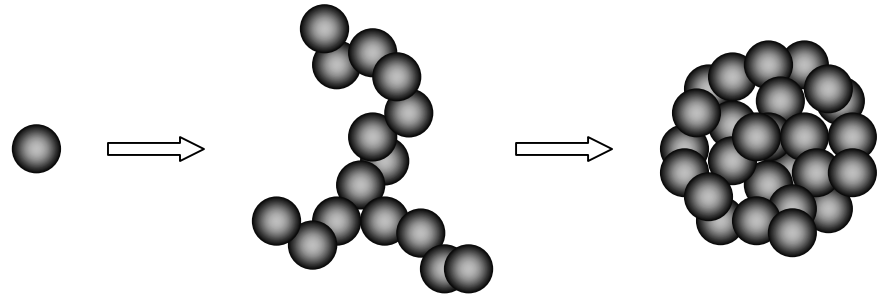

Fig. 1. Simplified scheme of the formation process of P-C aggregates.

It can be assumed that these agglomerates can be modeled as solid spheres with the effective radius R_p and the effective thermal conductivity k_p. Although this assumption can be questionable the structure of flame-generated aggregates shows some evidence of fractal-like properties. The latter can simplify their morphological description as it was demonstrated experimentally and supported by several theoretical studies (see, e.g., [4]).

3. Mathematical model

3.1 Thermo- and diffusiophoretic motion of P-C soot aggregates

In the present investigation P-C fractal aggregates are considered as compact spherical clusters with point contact of the soot particles. Since the diameter of the pores may not exceed the diameter of the particle (i.e., 10–30 nm) the aggregate is modeled as a solid sphere with completely diffusion reflection of the gas molecules at its surface (i.e., accommodation coefficient is equal to 1).
The velocity of a soot aggregate located in the field of temperature and concentration gradients can be expressed as the sum of three terms:

$$\mathbf{v} = \mathbf{u} + \mathbf{v}_{TP} + \mathbf{v}_{DP}, \tag{1}$$

where **u,** $\mathbf{v}_{TP}$ and $\mathbf{v}_{DP}$ are the gas, thermophoretic and diffusiophoretic velocities correspondingly. Well-established theory of thermophoresis (see, e.g., [5]) of large aerosol particles assumes that thermophoretic velocity can be obtained from the solution of the linearized system of steady-state Navier-Stokes and energy conservation equations with slip boundary conditions at the surface of the particle. In the case of moderately large aerosol particles the boundary conditions must include kinetic terms that are the functions of temperature jump, Knudsen number etc. This model can be used as long as: (i) the Stokes time τ_s is much less then the characteristic time scale for droplet combustion τ_{drop} (i.e., $\tau_s = \frac{2}{9}\frac{R_p^2}{\mu}\rho_p << \tau_{drop} = \frac{d_0^2}{K_b}$), and (ii) the nonlinear terms in momentum and energy conservation equations are much less then the linear terms. Since thermophoretic velocity is of the order of $v_{TP} \sim \frac{\mu}{\rho T_e}\left|\nabla T_e\right|$ it is easily seen that the condition for the validity of the model is $\left(R_p\left|\nabla T_e\right|\right)/T_e << 1$. Simple estimations show that for soot particle with the radius 1 μm and density $\rho = 1.8$ g/cm^3 moving in the vicinity of the burning n-heptane droplet of 0.4 mm diameter the Stokes time is of the order of 10^{-4} s whereas the characteristic time scale for droplet combustion is ~0.2 s. Since $\left(R_p\left|\nabla T_e\right|\right)/T_e \sim 10^{-3} << 1$ the above approach can be applied to model thermo-diffusiophoretic motion of flame-generated particles in the vicinity of the burning droplet.

The current theory of thermophoresis of solid particles in a gas at low Knudsen numbers yields the following expression for the thermophoretic velocity [5]

$$\mathbf{v}_{TP} = -f_T \frac{\mu}{\rho}\frac{\nabla T_e}{T_e}, \tag{2}$$

where

$$f_T = K_{TSL}\frac{1 + \mathrm{Kn}\cdot\Phi}{1 + k_p/(2k_e)} \tag{3}$$

and Φ is a function of the momentum accommodation coefficient α^*, energy accommodation coefficient ϵ and the ratio of thermal conductivity coefficients k_p/k_e. In the most general form, the function $\Phi\left(\epsilon, \alpha^*, k_p/k_e\right)$ reads [5]:

$$\Phi\left(\epsilon, \alpha^*, k_p/k_e\right) = A\left(\epsilon, \alpha^*\right)\frac{k_p}{k_e} + D\left(\epsilon, \alpha^*\right) + \frac{B\left(\epsilon, \alpha^*\right) + C\left(\epsilon, \alpha^*\right)\frac{k_p}{k_e}}{1 + k_p/2k_e}. \tag{4}$$

In the present study we adopted the coefficients *A*, *B*, *C*, and *D* determined in [6] (*A* = 2.26, *B* = 0.55, *C* = –2.18, *D* = –0.15, $\epsilon = \alpha^* = 1$). Due to high temperature differences thermal conductivity of the gaseous mixture in the neighborhood of a burning droplet varies significantly. However, simple estimations showed that the ratio k_p/k_e is ~ 10 with a small range of variation (approximately from 8.2 to 12.9). As can be seen from

Fig. 2 in this range the thermophoretic coefficient f_T (3) has only a weak dependence on k_p/k_e for Knudsen numbers in the range from 0.01 to 0.3.

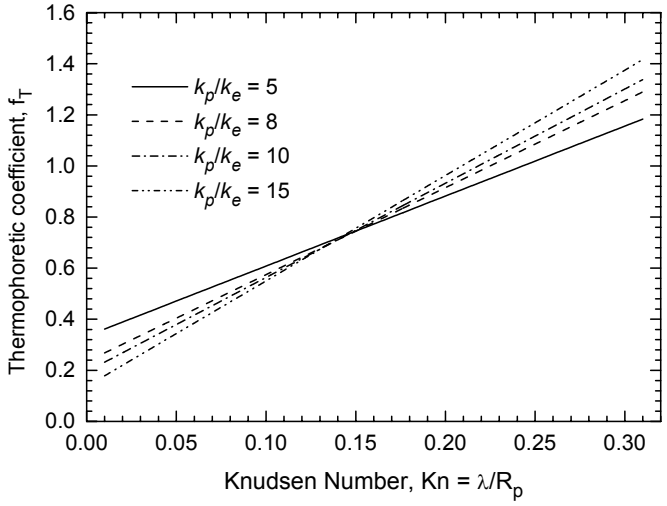

Fig . 2. Thermophoretic coefficient f_T vs. Knudsen number $\mathrm{Kn} = \lambda/R_p$ at various thermal conductivity ratios

The expression for the diffusiophoretic velocity of aerosol particle in multicomponent gaseous mixture was derived by Viehland & Mason [7]. In a frame attached to the droplet this expression reads:

$$\mathbf{v}_{DP} = \sum_{i=1}^{K-1} \frac{nD_i^*}{\rho} \left(\nabla y_i + \sum_{j=1}^{K} y_i y_j \alpha_{ij} \nabla \ln T_e \right), \tag{5}$$

where y_i and y_j are mole fractions of the *i*-th and *j*-th species correspondingly, $\alpha_{ij} = -\alpha_{ji}$ is multicomponent thermal diffusion factor, *n* is the total number density and the ρ is the total mass density of the gas. The coefficient D_i^* can be calculated using the method suggested by Viehland and Mason [7].

3.2 Model of the spherically symmetric droplet flame

In the present investigation spherically symmetric droplet flame was simulated using the system of dimensionless one-dimentional unsteady energy and mass conservation equations (6) –(7) [3]

$$\Psi \left[Y_i, \zeta_D, \rho D_i, M_i \left(\nu_i'' - \nu_i' \right), 0 \right] = 0 \tag{6}$$

$$\Psi \left[\theta_e, \zeta_T, k_e, Q M_F T_\infty^{-1}, 1 \right] = 0 . \tag{7}$$

The operator $\Psi \left[\phi, \beta, \gamma, \lambda, \chi \right]$ in equations (6)–(7) is defined as follows:

$$\Psi\ [\phi,\beta,\gamma,\lambda,\chi]=\xi^2\frac{\partial\phi}{\partial\tau}-x\xi\dot{\xi}\frac{\partial\phi}{\partial x}+u\frac{\xi R_0}{\alpha_\ell}\frac{\partial\phi}{\partial x}-\frac{\beta}{x^2}\frac{\partial}{\partial x}\left(x^2\gamma\frac{\partial\phi}{\partial x}\right)+$$
$$+\beta\xi R_0\left(\frac{\chi}{x^2T_\infty}\frac{\partial}{\partial x}\left(x^2\mathbf{Q}_R\cdot\mathbf{n}\right)-\lambda\xi R_0\dot{\omega}\right), \qquad (8)$$

where $u=u(x,\tau)$ is the gas velocity, $x=r/R(t)$, $\tau=\alpha_\ell t/R_0^2$ and $\theta_e=T_e/T_{e,\infty}$ are the dimensionless radial coordinate, time and gas temperature correspondingly, $\xi(\tau)=R(t)/R_0$ is the dimensionless droplet radius, ρ is the gas density, D_i is the diffusion coefficient of the *i*-th species, k_e is the gas thermal conductivity, c_p is the specific heat at a constant pressure , $\zeta_T=1/(\alpha_\ell\rho c_p)$ and $\zeta_D=\zeta_T c_p$, $\mathbf{Q}_R$ is the radiation flux vector, $\dot{\omega}$ is the mass production rate of the *i*-th species by gas phase one step chemical reaction given by the Arrhenius formula

$$\dot{\omega}=Z\left(\frac{\rho Y_F}{M_F}\right)^a\left(\frac{\rho Y_o}{M_o}\right)^b\exp\left(-\frac{E_a}{R_g\theta_e T_\infty}\right), \qquad (9)$$

where E_a is the activation energy, and Z is the pre-exponential constant, The gaseous phase velocity u and the rate of change of the droplet radius $\dot{\xi}$ can be determined as follows [9]

$$u(x,\tau)=-\frac{1}{x^2}\frac{\rho_\ell\alpha_\ell}{\rho R_0}\dot{\xi}(\tau), \qquad \dot{\xi}(\tau)=\frac{1}{\xi(\tau)}\frac{\rho_S D_{F,S}\left.\frac{\partial Y_F}{\partial x}\right|_{x=1}}{\rho_\ell\alpha_\ell(1-Y_{F,S})} \qquad (10)$$

In equations (10)–(11) α_ℓ is the liquid thermal diffusivity and subscript *S* denotes the value at the droplet surface. Initial and boundary conditions read:

$$\theta_e(0,x)=\theta_e^{(0)}(x), \qquad Y_i(0,x)=Y_i^{(0)}(x), \qquad (11)$$

$$\frac{1}{u}\frac{D_F}{\xi R_0}\left.\frac{\partial Y_F}{\partial x}\right|_{x=1}=(1-Y_F)|_{x=1}, \qquad \frac{1}{u}\frac{D_i}{\xi R_0}\left.\frac{\partial Y_i}{\partial x}\right|_{x=1}=Y_i|_{x=1} \qquad (i=\overline{2,K}), \qquad (12)$$

$$\frac{k_e}{k_\ell}\frac{1}{\xi}\left.\left(\frac{\partial\theta_e}{\partial x}\right)\right|_{x=1}=-\frac{L}{c_\ell T_\infty}\left.\frac{d\xi(\tau)}{d\tau}\right|_{x=1}+\frac{\xi}{3}\left.\frac{d\theta_e}{d\tau}\right|_{x=1}+\frac{R_0}{k_\ell T_\infty}(\mathbf{Q}_R\cdot\mathbf{n})|_{x=1}, \qquad (13)$$

$$Y_{F,S}(\theta_S)=\exp\left(-\frac{LM_F}{R_g T_b}\left(\frac{T_b}{\theta_S T_\infty}-1\right)\right). \qquad (14)$$

In equation (13) k_ℓ is coefficient of thermal conductivity of a liquid and c_ℓ is a specific heat of a liquid. At $x\to\infty$ and $\tau>0$, the soft boundary conditions at infinity are imposed:

$$\left.\frac{\partial\theta_e}{\partial x}\right|_{x\to\infty}=\left.\frac{\partial Y_i}{\partial x}\right|_{x\to\infty}=0 \qquad (i=\overline{1,K}) \qquad (15)$$

In order to determine the radiative heat flux from the flame it is assumed that the flame gases are optically thin. The system of unsteady nonlinear energy and mass conservation equations (6)–(7) formulated using inelastic approximation was solved numerically [2, 3], the temperature and concentration gradients in the vicinity of the droplet and the flame front were determined. The method of lines was employed to reduce the system of nonlinear partial parabolic differential equations to a system of ordinary differential equations.

4. Calculation of a mean diameter of P-C fractal soot aggregates

The drag force and thermophoretic and diffusiophoretic forces arising due to high temperature and concentration gradients affect transport of flame-generated particles inside and outside the flame. Soot particles are formed due to chemically controlled processes during combustion of hydrocarbon fuels and they can grow through the surface growth and collisional coagulation. The chemically controlled surface growth of soot particles is fairly fast. Thus, in the region between the droplet and the flame front as long as thermophoretic force is larger than diffusiophoretic and drag forces, the soot particles are propelled inward. The balance between the inwardly directed thermophoretic forces and outwardly directed drag and diffusiophoretic forces determines the location of the soot shell structure. Measurements based on thermophoretic sampling showed that flame-generated soot range from small aggregates (with the size of the order of 10 nm) near the start of soot formation, to large aggregates (with the size of the order of 1 μm) [8]. Using the calculated temperature and concentration distributions thermo and diffusiophoretic velocities of moderately large ($0.01 \lesssim \mathrm{Kn} \lesssim 0.3$) P-C fractal aggregates were calculated.

We performed numerical calculations of the dependence of the soot-shell-to-droplet diameter ratios (d_s/d) vs. mean radius of a soot particle (Fig. 3). As can be seen from this plot the soot-shell-to-droplet diameter ratios practically do not depend on time for the particles with the radii less then 0.6 μm.

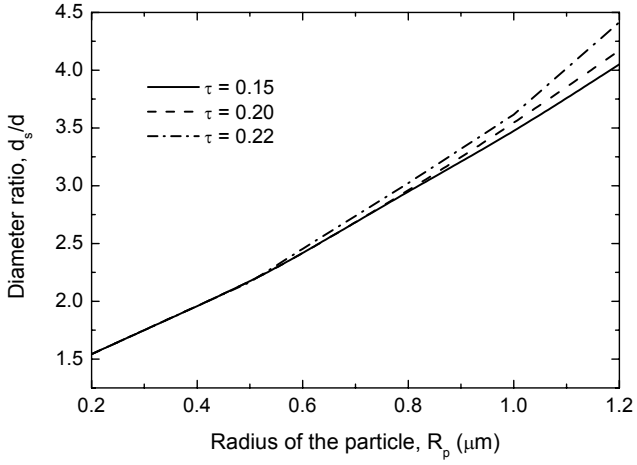

Fig. 3. Variations of the soot-shell-to-droplet diameters ratio vs. radius of P-C fractal soot aggregates at various instances of time.

Experimental measurements of soot-shell-to-droplet diameter ratios variation with time reported in [1] (see Fig. 4) showed that for n-heptane droplets soot-shell-to-droplet diameter ratios varied in the range from 2 to 3.5. As can be seen from Fig. 4, numerical results obtained in this study are consistent with the experimental observations for the soot particles with the radii in the range from 0.45 μm to 0.8 μm. Small increase of soot-shell-to-droplet diameter ratios during droplet combustion observed in [1] can be associated with the coagulation growth of soot aggregates.

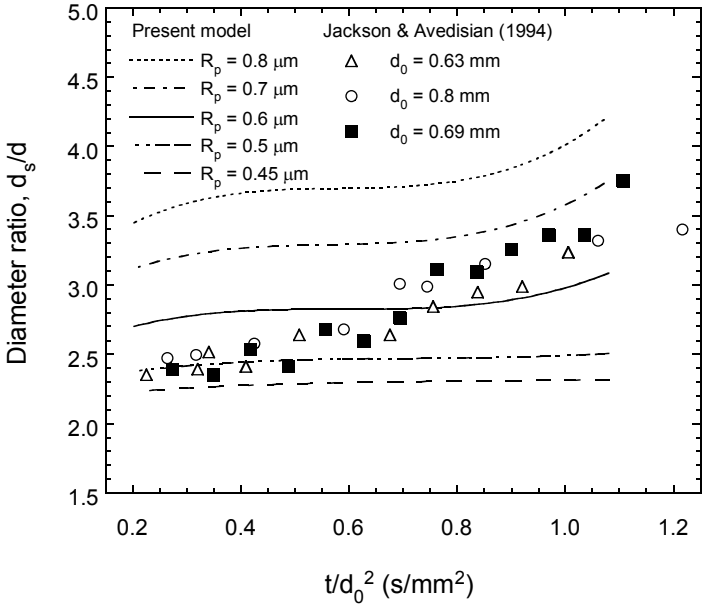

Fig. 4. Variation of soot-shell-to-droplet diameter ratio vs. time for various radii of P-C fractal soot aggregates R_p.

Comparing the dependences of soot-shell-to-droplet diameter ratio vs. time calculated using the present model with the experimental data obtained in [1] for 0.63mm n-heptane droplet allowed us to determine the time dependence of the mean soot aggregates radii (see Fig. 5).

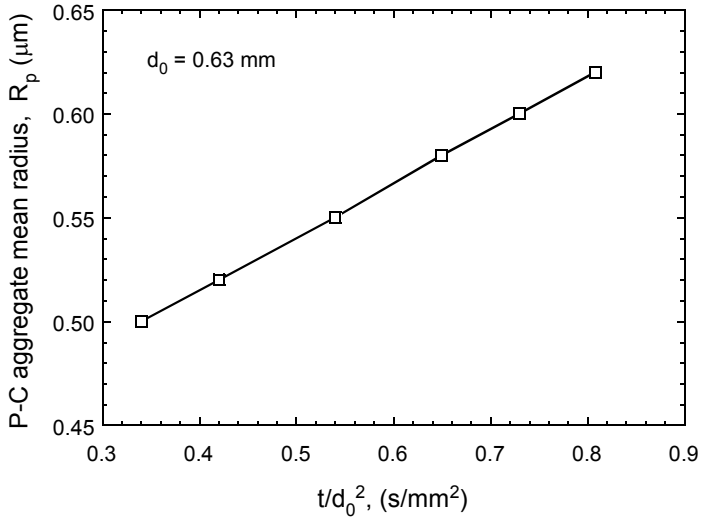

Fig. 5. Variation of the mean size of P-C fractal soot aggregates vs. time during droplet combustion.

Herewith the experimental data set was approximated by a linear function using the least squares method. As can be seen from Fig. 5 during combustion of n-heptane droplet with the initial diameter 0.63 mm the mean radius of the soot aggregates grows linearly with time in the range from 0.5 to 0.62 μm.
Thus experimental data on time variation of soot-shell-to-droplet diameter ratios allowed us to determine mean soot aggregates size growth with time during droplet burning using the inverse procedure and the developed model.

5. Conclusion

We performed numerical analysis of the effect of thermo- and diffusiophoretic forces on motion of flame-generated P-C fractal soot aggregates and formation of soot shell structure in the buoyant-free spherical droplet flames. The dependence of the soot-shell-to-droplet diameter ratios (d_s/d) on the radii of P-C soot aggregates was calculated numerically. It was shown that comparison of the experimental data on time variation of soot-shell-to-droplet diameter ratios [1] with the developed model and using the inverse procedure allowed us to predict mean soot aggregates size growth with time during droplet burning. Combining the obtained numerical results with the experimental data we found that during droplet combustion the mean soot aggregates size grows slowly and linearly with time.

References

[1] Jackson G S and Avedisian C T 1994 *Proc. R. Soc. Lond.* A **446** 255–276
[2] Ben-Dor G, Elperin T and Krasovitov B 2000 *J. Aerosol Sci*. **31** Supplement 1 S829–S830
[3] Ben-Dor G, Elperin T and Krasovitov B 2003 *Proc. R. Soc. Lond.* A **459** 677–703
[4] Brasil A M, Farias T L, Carvalho M G and Köylü U O 2001 *J. Aerosol Sci.* **32** 489–508
[5] Bakanov S P 1995 *J. Aerosol Sci.* **26**(1) 1–4
[6] Poddoskin A B, Yushkanov A A and Yalamov Yu I 1982 *Sov. Phys. Tech. Physics* **27**(11) 1383–1388
[7] Viehland L A and Mason E A. 1977 *J. Aerosol Sci*. **8** 381–385
[8] Köylü Ü Ö, Faeth G M, Farias T L and Carvalho M G 1995 *Combust. Flame*, **100**, 621–633
[9] Ben-Dor G, Elperin T and Krasovitov B 2003 *Heat and Mass Transfer*, **39**, 157–166